Journal of Trace Elements in Medicine and Biology 95 (2026) 127876

Contents lists available at ScienceDirect

Journal of Trace Elements in Medicine and Biology

journal homepage: www.elsevier.com/locate/jtemb

Transcriptomic response of human mesenchymal stromal cells exposed to Boron- and Molybdenum-substituted mesoporous bioactive glass nanoparticles

E. Kunisch [a], Q. Nawaz [b], T. Walker [a], T. Renkawitz [c], A.R. Boccaccini [b,*], F. Westhauser [c,**]

[a] Research Centre for Molecular and Regenerative Orthopaedics, Department of Orthopaedics, Heidelberg University Hospital, Heidelberg, Germany
[b] Institute of Biomaterials, University of Erlangen-Nuremberg, Erlangen, Germany
[c] Department of Orthopaedics, Regensburg University, Bad Abbach, Germany

ARTICLE INFO

Keywords:
Mesoporous bioactive glass nanoparticles
Molybdenum
Boron
Human bone marrow derived mesenchymal stromal cells
Whole genome analysis

ABSTRACT

Substitution of mesoporous bioactive glass nanoparticles (MBGNs; composition in mol%: 70 SiO_2- 30 CaO) with therapeutically active ions such as Molybdenum (Mo) ions modulates their osteogenic properties. To overcome the limited pro-angiogenic capability of MBGNs, a combination of Mo with pro-angiogenic boron (B) has been suggested. With regard to the missing knowledge about the global cellular response of bone marrow-derived human mesenchymal stromal cells (BMSCs) exposed to B- and Mo-MBGNs and their combinations, in this work a whole genome expression profiling was conducted to identify differentially expressed genes (DEGs) in BMSCs exposed to MBGNs, B-MBGNs, Mo-MBGNs and their combinations. Results were compared to those on untreated BMSCs. In MBGNs-exposed BMSCs, 93 DEGs were identified. Reactome pathway analysis revealed an overrepresentation of genes coding for enzymes of the cholesterol biosynthesis in all MBGNs-treated groups, whereas genes coding for molecules of extracellular matrix (ECM) proteoglycans and signaling of transforming growth factor-beta (TGF-β) family members were overrepresented after exposure to Mo-MBGNs. The DEGs of the identified Reactome pathways are tightly involved in modulating osteogenic differentiation. Further research is needed to clarify the exact role of the identified genes on the osteogenic potency of ion-substituted MBGNs adding fundamental information for the application of such nanoparticles in ionic medicine approaches.

1. Introduction

Since the introduction of the 45S5 bioactive glass (BG) composition (in wt%: 45.0SiO_2–24.5Na_2O–24.5CaO–6.0 P_2O_5) by Professor Larry Hench in the late 1960 s [1], a plethora of BG compositions has been designed to alter their processing and biological properties [2–4]. Usually, the newly developed BG compositions are thoroughly characterized with regard to their material properties [5]. This is mostly followed by in-vitro studies using different cell types to assess the cytocompatibility of the BGs. For a deeper characterization, the influence of BGs on osteogenic differentiation and angiogenic marker expression in osteoblast precursor cells is often analyzed. However, these expression analyses are restricted to a defined set of osteogenic and angiogenic markers. In case of osteogenic markers, mainly alkaline phosphatase (ALP), type I collagen alpha 1 (Coll1A1), Osteopontin (OPN), Osteocalcin (OCN) and the deposition of calcium and extracellular matrix are used as read out parameters [6–8]. To describe the angiogenic capacity of BGs, the angiogenic factors Vascular Endothelial Growth Factor (VEGF), Placental growth factor, Angiopoietin, and Angiogenin are used, sometimes complemented by tube formation assays using Human Umbilical Vein Endothelial Cells (HUVECs) and the chorioallantoic membrane (CAM) assay [8–10]. The analysis of these defined osteogenic and angiogenic parameters allows the assessment of the bone regeneration capacity of the developed BGs. However, this restricted view on a defined set of osteogenic and angiogenic molecules disregards the activation or suppression of additional genes and pathways by the newly developed BGs influencing the total osteogenic outcome. In order to overcome these limitations, the analysis of the whole gene expression pattern can be applied to provide broader insights into the global response of cells upon exposure to BGs.

* Correspondence to: Institute of Biomaterials, University of Erlangen-Nuremberg, 91058 Erlangen, Germany.
** Correspondence to: Department of Orthopaedics, Regensburg University, 93077 Bad Abbach, Germany.
E-mail addresses: aldo.boccaccini@fau.de (A.R. Boccaccini), Fabian.Westhauser@klinik.uni-regensburg.de (F. Westhauser).

https://doi.org/10.1016/j.jtemb.2026.127876
Received 4 February 2026; Received in revised form 1 April 2026; Accepted 13 April 2026
Available online 15 April 2026

Several studies already exist performing whole genome analysis on BG-exposed cells to identify differentially expressed genes (DEGs) modulated by the BGs [11–16]. The pioneering studies of Xynos et al. were the first implementing gene expression profiling to identify DEGs in the context of cells exposed to dissolution products of 45S5 BG [11,12]. They observed an upregulation of 60 RNA species including cell cycle regulators, transcription factors, and matrix components in human osteoblast exposed to the ionic extracts of 45S5 BG for 48 h and were the first ones to describe the tremendous impact of BG ionic dissolution products on cellular metabolism, growth, and differentiation [12]. Other studies analyzing the impact of different BG compositions on whole genome expression reported mainly the regulation of transcripts including osteoblast-related genes coding for growth factors and their associated molecules or receptors, extracellular matrix (ECM) protein components and degradation enzymes, transcription factors, other important osteoblast-associated markers, and genes involved in the mineralization process [13–15]. Although in these studies numerous DEGs were identified, at the end the focus was on those related to osteoblast differentiation, matrix modification and mineralization. In addition, no deeper analysis was performed to identify potential relations of DEGs using the respective databases for exploring gene interrelations [17–19]. To the authors' knowledge, only the study of Autefage et al. reported an unexpected upregulation of the isoprenoid pathway and the upregulation of genes coding for enzymes of this pathway in bone marrow-derived human mesenchymal stem cells (hMSCs) by the extract of strontium (Sr)-substituted 45S5 BG [16]. They subjected their obtained DEGs list to the Kyoto Encyclopedia of Genes and Genomes (KEGG) pathway analyses and found this unusual pathway for a biomaterial intended for bone tissue engineering (BTE).

As the development of new BG compositions continues, mesoporous bioactive glass nanoparticles (MBGNs) have gained much attention in BTE applications [20,21]. Their high porosity and specific surface area results in a superior bioactivity compared to conventional prepared melt-quench BGs [22]. Defined by their route of synthesis, they also allow the incorporation of various therapeutically active ions to tailor the composition towards specific (therapeutical) needs [23]. A wide range of ions have been already incorporated in MBGNs and have been proven to act pro-osteogenic and/or pro-angiogenic [23,24]. Recently, molybdenum (Mo) has been identified as a promising therapeutic ion to improve the osteogenic potency of MBGNs [25]. However, since Mo limits the angiogenic potency of MBGNs, the addition of pro-angiogenic boron (B) might compensate these limitations [25–27]. Currently, there is no study available analyzing the influence of MBGNs substituted with B or Mo or both on the whole genome expression pattern to identify genes and pathways involved in their osteogenic performance. Therefore, in the present study, bone marrow-derived human mesenchymal stromal cells (BMSCs) were exposed to MBGNs (nominal composition in mol%: 70 SiO_2, 30 CaO) substituted with 5 mol% MoO_3 or 5 mol% H_3BO_3 in exchange for CaO (Mo- or B-MBGNs, nominal composition in mol%: 70 SiO_2, 25 CaO, 5 MoO_3 or 5 B_2O_3) or defined combinations of B-MBGNs and Mo-MBGNs to perform whole genome expression profiling. Significance Analysis of Microarrays (SAM) was conducted to identify DEGs in the MBGNs-treated groups compared to unexposed BMSCs (control group). The individual DEG list of each MBGNs group was used to extract pathways and functional connections using over-representation analysis.

2. Materials and methods

2.1. MBGNs production and characterization

The MBGNs were synthesized using the micro-emulsion assisted sol-gel process, as described previously [28–30]. The synthesized MBGNs have been characterized by scanning electron microscopy (SEM) (FESEM, LEO 435VP, Karl Zeiss AG, Germany), energy-dispersive X-ray spectroscopy (EDX, LEO 435VP, Carl Zeiss™ AG), Fourier-transform infrared spectroscopy (FTIR, Nicolet 6700 FTIR spectrometer, Thermo ScientificTM, USA), and X-ray diffraction analysis (XRD, Rigaku Miniflex 600, Rigaku, Germany), as described in detail in previous publications [25,30]. The release of Mo and B ions in PBS from their respective synthesized MBGNs (Mo-MBGNs and B-MBGNs) was measured using Inductively coupled plasma optical emission spectroscopy (ICP-OES, Varian Vista MPX) and has been reported in our previous work [25,30]. The nominal composition of the MBGNs used in the present study is specified in Table 1. In case of Mo-substituted MBGNs, molybdenum chloride (Sigma-Aldrich) was used as molybdenum source, for B-substituted MBGNs boric acid was used. To obtain the combinations of B-MBGNs and Mo-MBGNs, defined amounts of both MBGNs were mixed together (wt%): 75% B-MBGNs/25% Mo-MBGNs (75B25Mo), 50% B-MBGNs/50% Mo-MBGNs (50B50Mo), 25% B-MBGNs/75% Mo-MBGNs (25B75Mo).

2.2. Experimental design of the study

To evaluate the influence of MBGNs, B-MBGNs, Mo-MBGNs, and the combinations of B-/Mo-MBGNs, BMSCs were cultivated in the presence of 1 mg/mL of the respective MBGNs (or combinations) for 2 days. This culture setting is used to assess the effects of the physical presence of MBGNs on the cells [31]. In addition, internalization of MBGNs by the cells plays a role in modulating the cellular behaviour by MBGNs exposure via endocytosis mechanisms and intracellular release of the therapeutic ions from the MBGNs [32–34]. Unstimulated cells cultivated on cell culture plastic served as control group. The influence on BMSCs cell number and viability was assessed by 4′,6-diamidino-2-phenylindole (DAPI) and fluorescein diacetate (FDA) staining and quantification to analyze the cytocompatibility of the different MBGNs treatments. For whole genome analysis, RNA of BMSCs treated with the different MBGNs were subjected to gene expression profiling. DEGs between the different MBGNs-treated groups and the control group were identified by SAM. Identified DEGs with a more than 1.5-fold differential mean expression between the unstimulated samples and samples exposed to the different MBGNs or their combinations were used for over-representation analysis to discover pathways. DEGs assigned to the identified pathways were validated by qPCR.

2.3. Study ethics and cell origin

BMSCs were isolated from bone marrow of 10 patients (5 male patients, mean age: 56.4 +/- 16.3; 5 female patients, mean age: 60.8 +/- 13.8) that underwent elective hip replacement surgery at Heidelberg Orthopaedic University Hospital. To minimize inter-individual variability cells were pooled in passage 1, as previously described [35]. Written consent from all patients was obtained prior to material collection. Cells were passaged at 80% confluency and stored in liquid nitrogen, the experiments were conducted with BMSCs in passage 4. Harvesting and utilization of BMSCs within the purpose of this study were approved by the responsible ethics committee of the Medical Faculty of the University of Heidelberg (S-340/2018).

2.4. BMSC isolation and cultivation

BMSCs were isolated using a density gradient centrifugation protocol as previously published [35–37]. Cells were cultivated in 0.1% gelatin (Sigma Aldrich, Steinheim, Germany) coated cell culture flasks

Table 1
Nominal composition of MBGNs.

	SiO_2 (mol%)	CaO (mol%)	B_2O_3 (mol%)	MoO_3 (mol%)
MBGNs	70	30	-	-
B-MBGNs	70	25	5	-
Mo-MBGNs	70	25	-	5

(Sarstedt, Nümbrecht, Germany) in expansion medium, consisting of Dulbecco's modified Eagle's medium (DMEM), high glucose, 12.5% fetal calf serum (FCS), 2 mM L-glutamine, 1% non-essential amino acids (NEAA), 50 μM β-mercaptoethanol (all Thermo Fisher Scientific, Langenselbold, Germany), 100 μg/mL penicillin/streptomycin (Sigma-Aldrich), and 4 ng/mL fibroblast growth factor 2 (Active Bioscience, Hamburg, Germany) under standard cell culture conditions (37°C and 5% CO_2 in a humidified atmosphere). To discard non-adherent cells, medium was exchanged after 24 h and subsequently three times per week.

2.5. Cell number quantification assay

Cell number was quantified by nuclear staining with DAPI (Thermo Fisher Scientific) as previously described [8]. Cells were washed with DPBS containing Ca^{2+} and Mg^{2+} (Thermo Fisher Scientific) and fixed using 70% ethanol (SERVA, Heidelberg, Germany) for 10 min. Thereafter cells were dried at 37°C followed by nuclear staining with DAPI (1 μg/mL) for 5 min. A washing step was performed to remove unbound dye and nuclear-bound DAPI was eluted. DAPI fluorescence intensity was measured using an aliquot of each sample at 355/460 nm (ex/em) in a microplate reader (OmegaReader, BMG Labtech, Ortenberg, Germany).

2.6. Quantitative and qualitative cell viability assay

BMSCs viability was determined using FDA as previously described [38]. In brief, BMSCs (0.2×10^5 cells/cm^2) were cultured in a 96-well plate in the presence of the different MBGNs or their combinations for 2 days. Cells cultivated on cell culture plastic served as control group. Thereafter, the medium was removed followed by a washing step with DPBS. After incubation of the cells with FDA (2 mg/mL FDA in DPBS) for 5 min at 37 °C, cells were lysed using 0.5% Triton-X-100 (Sigma-Aldrich). An aliquot of each cell lysate was transferred to a white microtiter plate. The fluorescence intensity was immediately determined at specific wavelengths for FDA, 485/535 nm (ex/em), using a fluorescence microplate reader (OmegaReader, BMG Labtech).

Cell morphology and viability were additionally analyzed by a fluorescence microscopy-based live/dead assay as previously described [39]. Cells (0.2×10^5 cells/cm^2) were washed once with DPBS containing Ca^{2+} and Mg^{2+} (Thermo Fisher Scientific), followed by incubation with 6 μM fluorescein diacetate (FDA; Sigma-Aldrich) in DPBS and propidium iodide (PI, Thermo Fisher Scientific; 0.2 μg/mL DPBS) for 2 min at 37°C for staining viable cells and dead cells, respectively. Thereafter, cells were washed with DPBS followed by imaging using a fluorescence microscope (Keyence BZ-X810; Keyence, Neu-Isenburg, Germany).

2.7. Microarray analysis

To identify DEGs and signaling pathways regulated by MBGNs in BMSCs, gene array analysis was performed. BMSCs (0.7×10^5 cells/cm^2) were cultivated in the presence of MBGNs for 2 days. Cells cultivated on cell culture plastic served as controls. Thereafter, total RNA was isolated using the RNeasy Mini Kit (Qiagen, Hilden, Germany) according the manufacturer's instructions and subjected to array hybridization. Quality control of total RNA, labeling, array hybridization, and microarray scanning were performed at the German Cancer Research Center Genomics Core Facility (Heidelberg, Germany). Gene expression profiling was performed using Affymetrix Human Clariom S Assay (Thermo Fisher Scientific). The fluorescence values from the cDNA array analysis were quantile normalized, log2 transformed and analyzed in Multiexperiment Viewer (MeV) 4.9.0 (TM4 Microarray-Software-Suite) [40]. DEGs between the groups were identified by unpaired Significance Analysis of Microarrays (SAM Version 1.0). The median false discovery rate (FDR) was set at < 0.05. Heat map visualization of the identified 1.5-fold up- or down regulated DEGs and cluster analysis was conducted using the Morpheus analysis software (Morpheus, https://software.broadinstitute.org/morpheus). Principal component analysis (PCA) was executed using the ClustVis Web Tool (ClustVis, https://biit.cs.ut.ee/clustvis/) [41]. PANTHER overrepresentation analysis was performed for the Reactome pathway annotation set submitting the individual list of DEGs with a more than 1.5-fold differential mean expression between the unstimulated samples and samples exposed to the different MBGNs or their combinations to the PANTHER software (http://pantherdb.org, Version 19.0, released 20 June 2020) [19,42]. As refence list, the whole genome list of Homo sapiens genes was used. Those DEGs of the identified Reactome pathways were selected for further analysis when they were found in three or more groups.

2.8. Validation of DEGs using qPCR

DEGs obtained by PANTHER overrepresentation analysis were selected for validation by quantitative real-time polymerase chain reaction (qPCR) when they had an appearance in three or more MBGNs-exposed groups. Total RNA was isolated from the cells using the RNeasy Mini Kit (Qiagen) according the manufacturer's instructions. Complementary DNA (cDNA) was synthesized using the High-Capacity RNA-to-cDNA Kit (Thermo Fisher Scientific). The PowerUp SYBR Green Master Mix (Thermo Fisher Scientific) and the primers (Sigma) listed in Table 2 were used to run the qPCR. For verification of primer specificity melting curve analysis and agarose gel electrophoresis was performed (data not shown). Relative expression level of the identified DEGs was calculated using the ΔCt method. Each target gene was related to Tyrosine 3-monooxygenase/tryptophan 5-monooxygenase activation protein zeta (YWHAZ) as endogenous control.

Table 2
Primer sequences used for validation of array data by qPCR. tyrosine 3-monooxygenase/tryptophan 5-monooxygenase activation protein zeta (YWHAZ; reference gene), lanosterol 14α-demethylase (CYP51A1), 7-dehydrocholesterol reductase (DHCR7), 24-dehydrocholesterol reductase (DHCR24), 3-hydroxy-3-methylglutaryl-CoA synthase (HMGCS1), insulin-induced gene 1 (INSIG1), sterol-C4-methyl oxidase (MSMO1), Asporin (ASPN), Inhibin beta A chain (INHBA), Plasminogen activator inhibitor 1 (SERPINE1), transforming growth factor-β2 (TGFB2), transforming growth factor-β3 (TGFB3), transforming growth factor-β receptor3 (TGFBR3), sterol regulatory element-binding protein 1 (SREBP), extracellular matrix (ECM), transforming growth factor beta (TGFB).

Gene	Primer sequence: 5'→3' (FW: forward, REV: reverse)	Function
YWHAZ	FW: TGCTTGCATCCCACAGACTA REV: AGGCAGACAATGACAGACCA	Reference gene
CYP51A1	FW: CTACAGTCGCCTGACAACAC REV: CCACTTTCTCCCCAACTCTC	Cholesterol biosynthesis
DHCR7	FW: ACGTAGGAGGCATCCAGGAG REV: GCGAGAACCAGGACAGGAGA	
DHCR24	FW: CTGCCGCTCTCGCTTATCTTC REV: TCTTGCTACCCTGCTCCTTCC	
HMGCS1	FW: AAGTCACACAAGATGCTACACCG REV: TCAGCGAAGACATCTGGTGCCA	
INSIG1	FW: TAACCACGCCAGTGCTAAAT REV: CCACTTCTGGAACGATCAAA	Regulation of cholesterol biosynthesis by SREBP
MSMO1	FW: ATCATGAGTTTCAGGCTCCATT REV: AAGCACGATTCCAATGAAAAAT	Cholesterol biosynthesis
ASPN	FW: TTTAGCCCTTCACACATCGC REV: TGGTTGGGACTGAGGTCAAA	ECM proteoglycans
INHBA	FW: CCTCGGAGATCATCACGTTT REV: CCCTTTAAGCCCACTTCCTC	Signaling by activin
SERPINE1	FW: GCAGCAGATTCAAGCAGCTAT REV: CTCCTTGTACAGATGCCG	Dissolution of fibrin clots
TGFB2	FW: GGCTCAGTGGGCAGCTTGT REV: GCTCAATCCGTTGTTCAGGC	TGFB receptor signaling activates SMADs
TGFB3	FW: CCCAGCTCTAAGCGGAATGAG REV: GCGCTGTTTGGCAATGTG	
TGFBR3	FW: TGGGGTCTCCAGACTGTTTTT REV: CTGCTCCATACTCTTTTCCGGG	Signaling by TGFB family members

2.9. Quantification of calcium and phosphate

With regard of an influence of calcium and phosphate on cell behavior and gene expression, the concentration of both were measured in the cell culture supernatants. Calcium quantification was performed with the Infinity Calcium Arsenazo III reagents according to the manufacturer's instructions (Thermo Fisher Scientific) using aliquots of undiluted supernatants [43]. The Phosphate concentration in supernatants was analyzed with a malachite green reaction solution [44]. Diluted sample or standard and malachite green solution were combined in a 96-well microtiter plate. Absorbance was immediately measured at 650 nm with an ELISA-Reader (Omega Reader, BMG Labtech). Calcium and phosphate concentrations in the supernatants were calculated as mM using serial dilutions of $CaCl_2$ x 2 H_2O and KH_2PO_4, respectively (both Carl Roth).

2.10. Statistics

IBM SPSS (Version 25; IBM, Armonk, NY, USA) was used for statistical evaluation. Significances were calculated using the non-parametric Kruskal-Wallis test followed by the Mann-Whitney *U* test. Parameters showing statistically significant differences among different groups in

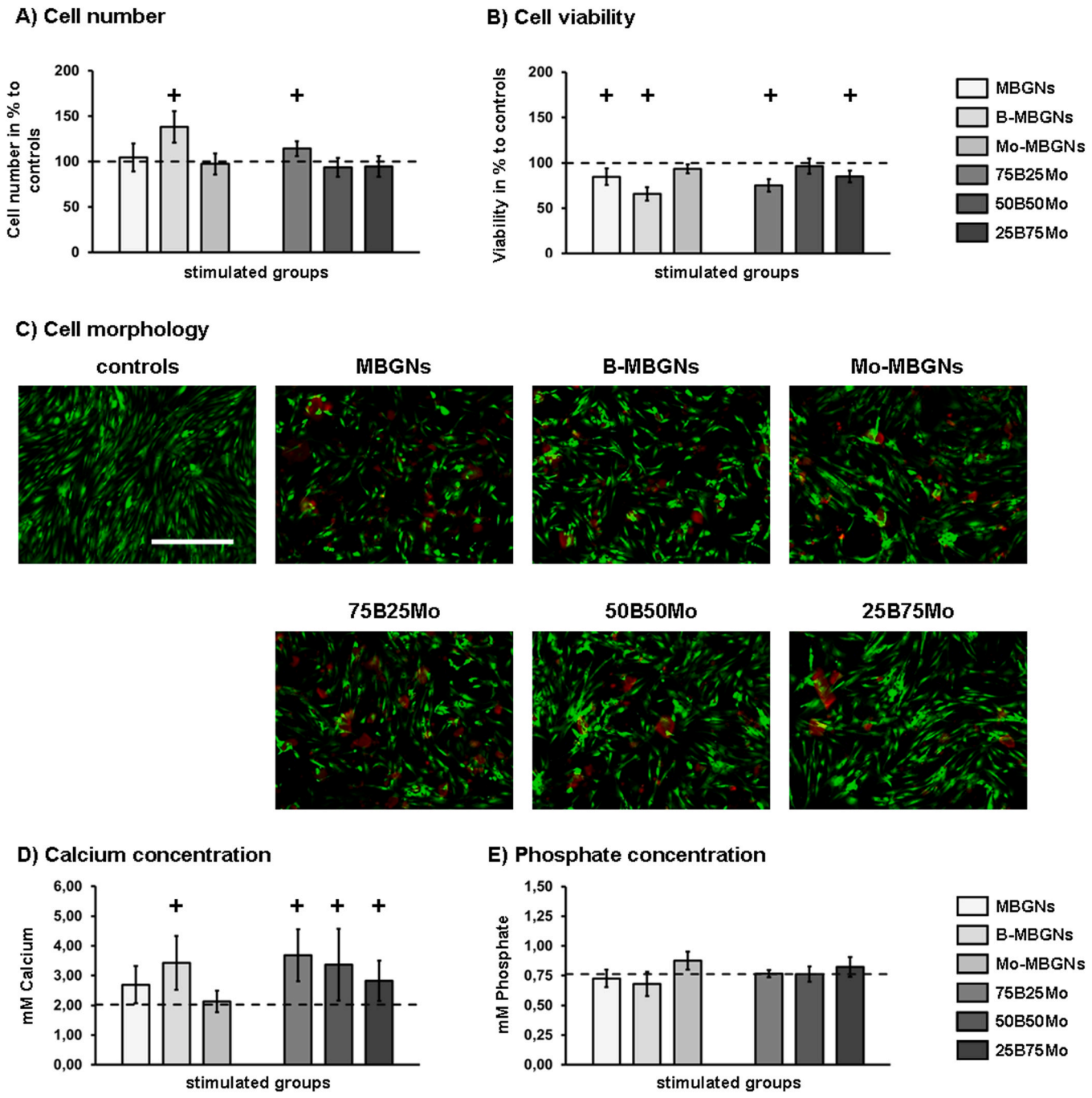

Fig. 1. Cytocompatibility, Calcium and Phosphate concentrations in the different culture settings: BMSCs were cultivated in the presence of the respective MBGNs and their combinations for two days. Thereafter A) cell number was assessed by DAPI quantification. B) Cell viability was analyzed by FDA measurement. C) Cell morphology was visualized by FDA staining. D) Calcium and E) phosphate concentration in the supernatants of the cells. + $p < 0,05$ Mann-Whitney U Test versus control. Dotted line in A), B), D), and E) indicates the control group (set 100% in A) and B)). Scale bar in C) refers to 500 μm.

the Kruskal-Wallis multigroup test were then analyzed for significant differences between individual groups. Differences were considered statistically significant for $p < 0.05$. All results are expressed as means ± standard deviation (SD). Graphs were designed using Microsoft Excel (Microsoft, Redmond, WA, USA). Micro array analysis was performed in n = 3 biological replicates, all other measurement in n = 6 biological replicates.

3. Results

3.1. Characterization of the MBGNs

The characterization of the MBGNs used in the present study has been extensively described in our previous publications [25,30]. In brief, SEM images of the synthesized MBGNs (non-doped and doped) showed that the MBGNs particles had a spherical morphology, which was not affected by the incorporation of boron and molybdenum ions into the silica network. EDX spectroscopy confirmed the presence of silicon, calcium and molybdenum in Mo-MBGNs. FTIR spectroscopy identified the three signature peaks for the silica network in the produced MBGNs around 790 cm^{-1}, 1100 cm^{-1}, and 473 cm^{-1} [45,46]. The correct incorporation of boron and molybdenum ions into the silica network was validated by the appearance of typical peaks for boron bonding at 925 cm^{-1} and 1400 cm^{-1} in B-MBGNs spectra and for Mo–O-Mo bonds at 898 cm^{-1} in the spectra of Mo-MBGNs [6,47]. The amorphous character of MBGNs and B-MBGNs was confirmed by XRD analysis. However, crystalline peaks in Mo-MBGNs XRD patterns points to the existence of a second phase ($CaMoO_4$) [47]. Measurement of the Mo and B release by ICP-OES revealed a continuous release of both ions from MBGNs although the B release was lower compared to the Mo release [25,30]. Since SEM images of the synthesized MBGNs show no differences in the monodispersity and spherical nature of the particles, any differences in gene expression profile and identified pathways can be attributed to the release of ions by the MBGNs.

3.2. Cytocompatibility of the MBGNs and their combinations

Cultivation of BMSCs in the presence of the different MBGNs or their combinations significantly increased the cell number in the B-MBGNs- and 75B25Mo-incubated groups compared to the control (Fig. 1A). In all other groups, no significant difference was observed compared to the control group. The cell viability was significantly reduced by cultivating BMSCs in the presence of MBGNs, B-MBGNs, and the 75B25Mo and 25B75Mo combinations in comparison to the control group (Fig. 1B). Qualitative growth pattern and morphology visualized by FDA staining revealed an elongated fibroblast-like growth pattern in all groups (Fig. 1C). However, cell density appeared less dense in the MBGNs-treated groups compared to the control group.

The calcium concentration in the supernatant of BMSCs exposed to B-MBGNs or to the B-/Mo-MBGNs combinations was significantly higher compared to that of the control group (Fig. 1D). No significant differences were observed in the phosphate concentration between the different groups (Fig. 1E).

3.3. Identification of DEGs in BMSCs co-cultivated with MBGNs and their combinations by global gene expression analysis

Using SAM analysis, in total 93 DEGs were identified being 1.5-fold up- or downregulated in the groups incubated with MBGNs in comparison to the control group. Heatmap analysis of the identified DEGs of each MBGNs group showed a differential expression pattern between the analyzed groups (Fig. 2A).

Cluster analysis detected two main clusters, (i) the controls and (ii) the samples treated with the different MBGNs (Fig. 2B). In the MBGNs cluster, two clusters were separated, one containing the MBGNs stimulated samples and the B-MBGNs samples and the second one containing the Mo-MBGNs samples and the samples stimulated with the combinations of Mo-/B-MBGNs. Whereas the MBGNs samples and the B-MBGNs samples were clearly distinguished by their expression profile, the samples incubated with the Mo-MBGNs and Mo-/B-MBGNs combinations were poorly discriminated by their DEGs expression pattern. PCA of the expression values of identified DEGs validated the results of cluster analysis (Fig. 2C). A high degree of separation along PC1 (49.5%) was observed between the control samples and the MBGNs-treated samples. In addition, the Mo-MBGNs samples were clearly clustered from the MBGNs and B-MBGNs samples (along PC2, 28.9%). Between the Mo-MBGNs samples and the samples of B-/Mo-MBGNs combinations as well as the MBGNs and B-MBGNs samples minor expression profile shifts were observed.

Classifying the individual DEGs for each group with PANTHER overrepresentation analysis for the Reactome pathway annotation set, three main Reactome pathways were detected (Fig. 2D): Cholesterol biosynthesis, ECM proteoglycans, and signaling by transforming growth factor beta (TGFB) family members. Additionally, Table 3 provides an overview of the impact of exposure to the different MBGNs-settings on these major pathways. While overrepresentation of cholesterol biosynthesis was assigned to all MBGNs groups, ECM proteoglycans, and signaling by TGFB family members was allocated to DEGs of the groups incubated with Mo-MBGNs and the combinations (Table 3). DEGs belonging to cholesterol biosynthesis, namely CYP51A1, DHCR7, HMGCS1, and MSMO1, were higher expressed (> 1.5-fold) in BMSCs exposed to the different MBGNs or the combinations compared to the control group (Fig. 2E). For DEGs of the ECM proteoglycans and signaling by TGFB familiy members, ASPN and TGFBR3 were higher expressed compared to controls (> 1.5-fold; Fig. 2F). The RNA level of INHBA, SERPINE1, TGFB2, and TGFB3 was lower compared to controls.

3.4. Validation of the DEGs identified by whole genome analysis using qPCR

The RNA levels of DEGs belonging to the cholesterol biosynthesis pathway were numerically (CYP51A1 and HMGCs1) or significantly (DHCR7 and MSMO1) upregulated (> 1.5-fold) in the MBGNs-treated groups compared to the untreated control group (Fig. 3A-D). The CYP51A1 RNA level was numerically higher in all groups cultivated in the presence of MBGNs compared to control group with no significant differences between the MBGNs-treated groups (Fig. 3A). For DHCR7, the RNA expression level was significantly higher in all MBGNs-incubated groups compared to controls (Fig. 3B). A significantly higher DHCR7 RNA level was observed in the B-MBGNs-, Mo-MBGNs-, and the 75B25Mo-treated groups compared to the group cultivated with MBGNs. In addition, the DHCR7 RNA expression was significantly higher in the groups cultivated with B-MBGNs and Mo-MBGNs compared with the 50B50Mo group. The HMGCS1 RNA expression level was numerically higher in all MBGNs-treated groups compared to controls except for the 50B50Mo group with no significant difference between the MBGNs-cultivated groups (Fig. 3C). A significantly higher MSMO1 RNA level was detected in cells incubated with B-MBGNs, Mo-MBGNs, 75B25Mo, or 25B75Mo combination compared to control cells (Fig. 3D). As observed for DHCR7, the MSMO1 RNA expression was significantly higher in the groups cultivated with B-MBGNs, Mo-MBGNs, or the 75B25Mo combination compared with the MBGNs group. A significantly higher MSMO1 RNA expression was detected in cells cultivated with B-MBGNs and Mo-MBGNs compared with the 50B50Mo-treated cells. Two additional genes involved in cholesterol biosynthesis, DHCR24 and INSIG1, were analyzed for their expression in the MBGNs-treated cells. The DHCR24 RNA expression level was significantly higher in BMSCs cultivated in the presence of Mo-MBGNs and the 75B25Mo and 25B75Mo combination compared to controls (Fig. 3E). Incubation of cells with Mo-MBGNs significantly increased DHCR24 RNA level in comparison to the MBGNs, B-MBGNs, and the 75B25Mo group. For INSIG1, the RNA level of all MBGNs groups was significantly higher

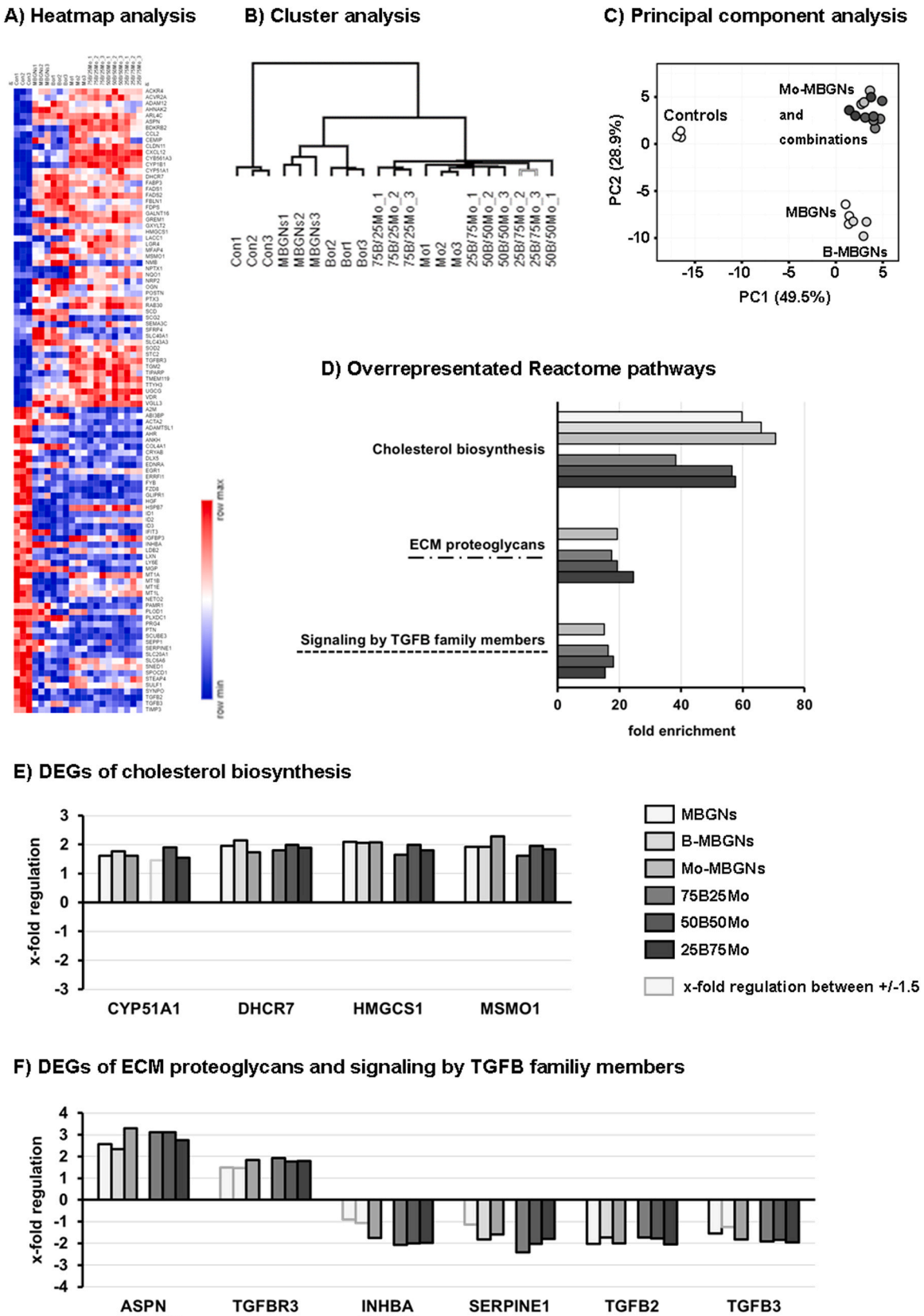

Fig. 2. Changes of BMSCs global gene expression mediated by co-cultivation with MBGNs, B-MBGNs, Mo-MBGNs, and their combinations. A) Heatmap of the identified DEGs of the samples of each group. B) Cluster analysis of the samples of each group according to their DEGs expression. C) Principle component analysis based on DEGs expression of the different groups. D) Identified overrepresented Reactome pathways. E) and F) identified DEGs allocated to the overrepresented Reactome pathways. DEGs of ECM proteoglycans and Signaling by TGFB family have been merged in F) since DEGs of both pathways were nearly identical. Differential DEGs between both Reactome pathways are marked by different underlines.

Table 3
Summarized results of DEGs identified by Panther analysis/Reactome pathways. ↑ > 1.5-fold upregulation, ↓ < -1.5-fold downregulation; - regulation between + /- 1.5; grey shaded – groups were not assigned to any of the identified Reactome pathways.

		Compared to controls					
		MBGNs	B-MBGNs	Mo-MBGNs	75B25Mo	50B50Mo	25B75Mo
Cholesterol biosynthesis	CYP51A1	↑	↑	↑	-	↑	↑
	DHCR7	↑	↑	↑	↑	↑	↑
	HMGCS1	↑	↑	↑	↑	↑	↑
	MSMO1	↑	↑	↑	↑	↑	↑
ECM proteoglycans/ Signaling by TGFB family members	TGFBR3	-	-	↑	↑	↑	↑
	SERPINE1	-	↓	↓	↓	↓	↓
	TGFB2	↓	↓	↓	↓	↓	↓
	TGFB3	↓	-	↓	↓	↓	↓
ECM proteoglycans	ASPN	↑	↑	↑	↑	↑	↑
TGFB family	INHBA	-	-	↓	↓	↓	↓

compared to controls except for the B-MBGNs-treated group (Fig. 3F). A significantly higher INSIG1 RNA level was detected in BMSCs exposed to Mo-MBGNs compared to the MBGNs- and the B-MBGNs-treated cells.

Validation of DEGs belonging to ECM proteoglycans and signaling by TGFB family members confirmed the array results with an upregulated expression of ASPN and TGFBR3 and a downregulated expression of INHBA, SERPINE1, TGFB2, and TGFB3 mainly in the groups incubated with Mo-MBGNs. The ASPN RNA level was significantly higher in all MBGNs-treated groups compared to the control group (Fig. 3G). A significantly higher ASPN RNA level was detected in BMSCs exposed to Mo-MBGNs compared to the 50B50Mo group and in cells incubated with the 25B75Mo combination compared to the B-MBGNs and the 50B/50Mo group. The TGFBR3 RNA level was significantly higher only in the Mo-MBGNs group compared to the control group (Fig. 3H). The INHBA RNA level was significantly decreased in BMSCs exposed to Mo-MBGNs, the 75B25Mo, and 50B50Mo combinations compared to the control group (Fig. 3I). Cells incubated with the 75B25Mo or 50B50Mo combination had a significantly decreased INHBA RNA level compared to MBGNs- and B-MBGNs-treated cells. For SERPINE1, a significantly lower RNA level was detected in the B-MBGNs-, the 75B25Mo- and the 50B/50Mo-treated groups compared to the control group (Fig. 3J). The SERPINE1 RNA level was significantly diminished in BMSCS exposed to the 75B25Mo combination compared to MBGNs-, B-MBGNs-, Mo-MBGNs-, and 25B75Mo-treated group. Also, treatment with the 50B50Mo significantly reduced the SERPINE1 RNA level in the cells compared to the MBGNs- and 25B75Mo-treated group. The TGFB2 RNA level was solely numerically lower in all MBGNs-treated groups compared to the control group except for the 25B75Mo-treated group with no significant difference between the MBGNs-incubated groups (Fig. 3K). For TGFB3, a significantly decreased RNA level was observed in all MBGNs group compared to the control with no significant difference between the groups exposed to the different MBGNs and their combinations except for the group cultivated in the presence of B-MBGNs (Fig. 3L).

4. Discussion

Numerous bioactive ions have been already incorporated in MBGNs to improve their osteogenic and/or angiogenic potency [23,24]. Mo has been recently identified as therapeutic ion to improve the osteogenic potency of MBGNs [25,48]. Regarding the restricted pro-angiogenic capability of Mo-MBGNs, the addition of a pro-angiogenic ion to the MBGN composition, e.g. Boron, has been considered to improve the nanoparticles' angiogenic potential [25]. Viceversa, this combinatory approach also allows to compensate for the known limited osteogenic capacity of B-MBGNs [6]. Although the osteogenic and angiogenic capabilities of Mo- and B-MBGNs have already been described [6,25], their impact on the whole genome expression has not been analyzed so far. Therefore, the present study was conducted to reveal genes and pathways stimulated by MBGNs substituted with B and Mo and the combination of B- and Mo-MBGNs by whole genome analysis using BMSCs. In total, 93 1.5-fold up- or downregulated DEGs were identified in all groups. Using the individual DEGs list, genes coding for enzymes or molecules of the cholesterol biosynthesis and ECM proteoglycans, and signaling by TGFB family members were identified as overrepresented. The expression pattern of DEGs belonging to the cholesterol biosynthesis, ECM proteoglycans and signaling by TGFB family members were validated by qPCR clearly showing the superiority of Mo-MBGNs over MBGNs or B-MBGNs in modulating the expression of the DEGs.

To exclude any harmful effects of the B- and Mo-MBGNs and their combinations on BMSCs, cytocompatibility testing was performed before cell culture experiments for gene array analysis were conducted. Cocultivation of BMSCs with MBGNs, B-MBGNs, and the 75B25Mo- or 25B75Mo-combinations reduced the viability of the cells up to 65% (B-MBGNs group). A reduction of cell viability by incubation with MBGNs and B-MBGNs was also reported by Ege et al. [29]. In their study, incubation of C2C12 cells with MBGNs or B-MBGNs reduced cell viability. In the present study, Mo-MBGNs had no negative impact on cell viability after two days. This is in contrast to previously published data [25,47].

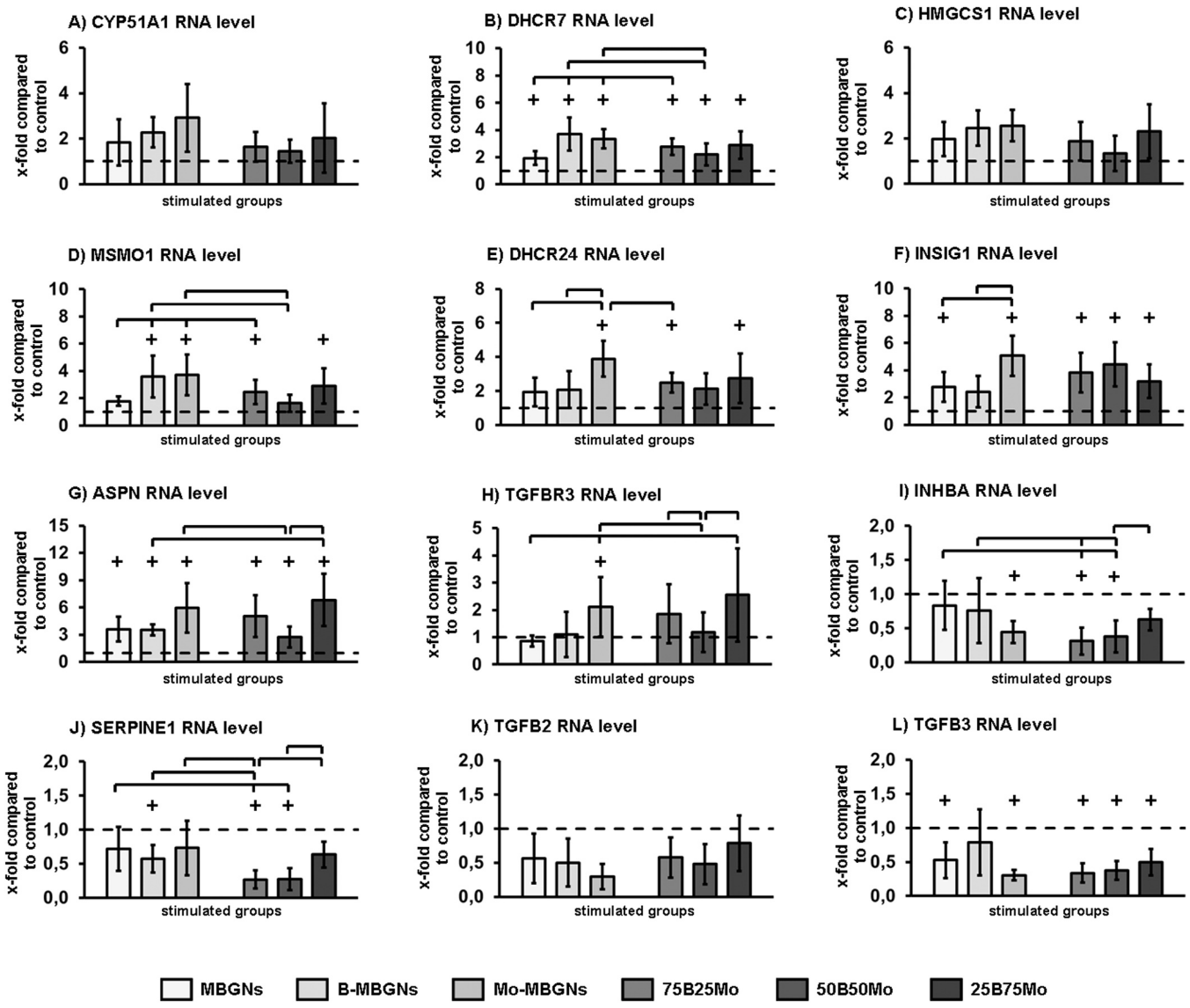

Fig. 3. Validation of DEGs of cholesterol biosynthesis and ECM proteoglycans and signaling by TGFB family members. A) CYP51A1, B) HMGCS1, C) DHCR7, D), MSMO1 G) ASPN, H) TGFBR3, I) INHBA, J) SERPINE1, K) TGFB2, and L) TGFB3. In the cholesterol biosynthesis group, the RNA level of E) DHCR24 and F) INSIG1 were additionally analyzed. Both genes were not identified as DEGs by SAM analysis, but were detected as upregulated > 1.5-fold in the MBGNs groups by whole genome analysis. + $p < 0,05$ Mann-Whitney U Test versus control. Between the MBGNs-treated groups significant differences were indicated with brackets. Dotted line in all figures indicates the control group.

Both studies reported a decrease of cell viability by exposure of the cells to Mo-MBGNs at early time points, after 3 days of incubation [25] and after 1 and 3 days of incubation, respectively [47]. However, in the study of Niu et al., the decreasing effects of Mo-MBGNs were more pronounced on day 3 compared to day 1 pointing towards a time-dependent effect of Mo-MBGNs on viability. No negative effect of the MBGNs on cell number was observed. Noteworthy, the B-MBGNs even significantly increased the cell number. This result can be explained by a higher calcium content in the supernatant of B-MBGNs cultures. Calcium is known to increase cell proliferation [49,50]. Therefore, in summary, the MBGNs and their combinations showed good cytocompatibility in a concentration of 1 mg/mL.

In the present study, genes of the cholesterol biosynthesis and ECM proteoglycans, and signaling by TGF-β family pathways were identified as overrepresented using the individual DEGs lists for each MBGNs-exposed group. For genes encoding enzymes of the cholesterol biosynthesis, namely CYP51A1, DHCR7, HMGCS1, MSMO1, DHCR24, and INSIG1, an upregulation was observed in all MBGNs-treated groups. The enzymes coded by the identified genes CYP51A1, DHCR7, HMGCS1, MSMO1, DHCR24 catalyze different steps of the cholesterol biosynthesis [51]. INSIG1 together with INSIG2 regulates the cholesterol synthesis [51,52]. An increase in the expression of genes coding for enzymes of cholesterol biosynthesis pathway seems to be unusual for a biomaterial which is intended to be used in BTE and therefore should promote the expression of osteogenic genes. However, the result of the present study is in agreement with the findings reported by Autefage et al. [16]. In their study, hMSCs were incubated with extracts of 45S5 BG substituted with increasing amount of Sr. Whole genome expression profiling identified a significant upregulation of genes encoding enzymes of the mevalonate and steroid pathway by the extracts of Sr-containing BGs compared to the 45S5 BG and the control, e.g. FDPS, HMGCS1, DHCR7, and MSMO1. In the present study, also the ion-substituted MBGNs, especially the Mo substitution, had a stronger effect on gene expression compared to the MBGNs underlining the benefit of ion-doped MBGNs on gene expression and metabolism.

Cholesterol and the enzymes of its biosynthesis have been already

examined in the context of osteogenic differentiation. Several studies exist pointing towards an osteogenesis-regulating function [51,53–55]. Exposure of murine mesenchymal stem cells to cholesterol (5 μg/mL, 10 μg/mL, 15 μg/mL) under osteogenic conditions increased the expression of several osteogenic markers (BMP2, RUNX2, ALP, and OCN) and the mineralization capacity [53]. In contrast, a higher concentration of cholesterol (25 μg/mL, 50 μg/mL) inhibited the expression of ALP, Col1A1, BMP2, and RUNX2 [54]. In the study of Suzuki et al., deletion of DHCR7 significantly increased the expression of several osteogenic markers (Col1A1, OCN, Osteonectin (SPARC), Osterix (SP7)) in frontal bone during embryonic development [55]. Conversely, the deletion of INSIG1/2 resulted in the reduction of Col1A1, OCN, SPARC, SP7, OPN. The central role of cholesterol in osteogenesis is further supported by the observation that knock out of genes coding for enzymes of the cholesterol biosynthesis in mice results in defects in bone formation and/or homeostasis [51]. There are several mechanisms explaining the essential role of cholesterol in cellular function and also in osteogenesis. Cholesterol is enriched in lipid rafts, dynamic microdomains of the cellular membrane playing a role in cell signalling and intracellular transport [56]. Cholesterol is also needed for the proper formation of the primary cilia of cells [55]. This cellular structure transduces mechanical cues and signals from morphogens and growth factors. Primary cilia are also needed for an adequate function of WNT and Hedgehog signalling, which are known to be essential for osteogenesis [55]. Therefore, cholesterol is closely linked to osteogenesis. Thus, the observed modulation of the enzymes of the cholesterol biosynthesis by MBGNs in the present study (or by other BGs [16]) can have an impact on the osteogenic outcome when applied to BTE.

While the DEGs of the cholesterol biosynthesis were regulated in all MBGNs-groups, the DEGs of the ECM proteoglycans and signaling by TGF-β family members were predominantly identified in the Mo-MBGNs-stimulated groups. Both clusters included nearly the same DEGs (TGFBR3, SERPINE1, TGFB2, TGFB3) with ASPN belonging to ECM proteoglycans and INHBA to signaling by TGFB family members. To the best knowledge of the authors these molecules have not yet been examined in the context of BGs for BTE. As observed for the genes coding enzymes of the cholesterol biosynthesis, Mo-MBGNs and B-/Mo-MBGNs combinations had the most pronounced impact on the RNA level of these genes further underlining the superiority of Mo-substituted MBGNs and the combinations over MBGNs or B-MBGNs.

The proteins coded by the identified DEGs of the ECM proteoglycans and TGF-β family members are strongly related to osteogenesis, bone regeneration, and bone related diseases and their expression and physiological function is tightly connected [57–60]. ASPN, an extracellular matrix protein belonging to the small leucine-rich repeat proteoglycan family of proteins, is a known factor in osteoarthritis susceptibility and progression [60,61]. ASPN is also involved in the outcome of osteogenic differentiation [62–64]. Overexpression of ASPN in rat BMSCs suppressed osteogenic marker expression, namely RUNX2, SP7, ALP, bone sialoprotein, and OCN, under osteogenic conditions [62]. Conversely, ASPN knock down cells had a higher expression of RUNX2, SP7, ALP, and OPN [63,64]. SERPINE1, also known as Plasminogen activator inhibitor-1 (PAI-1), is an important regulator of the plasminogen/-plasmin system and therefore regulates tissue remodeling and growth factor release from the extracellular matrix [59,65]. SERPINE1/PAI-1 deficiency has been shown to reduce the expression of osteogenic marker (BMP2, ALP, SP7, OCN) in murine MSCs [66]. As for cholesterol, proteins coded by the identified genes of ECM proteoglycans and signaling by TGF-β family members interfere and regulate osteogenic differentiation at multiple steps. Therefore, more attention should be paid to the evaluation of these genes in the context of BGs and BTE. The exact role of the effects of MBGNs on gene expression of the identified DEGs (increased expression in the case of ASPN and TGFBR3, suppressed in the case of INHBA, SERPINE1, TGFB2, and TGFB3) and the mode of action of MBGNs (physical contact and/or internalization of MBGNs by the cells) on the osteogenic outcome of osteoblast precursor cells needs to be evaluated in detail in further studies.

Besides the identification of DEGs and pathways, data from whole genome analyses might also help to evaluate the benefit of ion substitution by the shift of the gene expression profile induced by the alteration of BG compositions. In the present study, heatmap analysis, cluster analysis and PCA clearly distinguished differences between the control samples and the MBGNs groups. In addition, the gene expression profile of MBGNs and B-MBGNs samples were also clearly separated from the expression patterns in Mo-MBGNs.

5. Conclusions

In the present study, whole genome expression profiling was performed in BMSCs exposed to MBGNs, B-MBGNs, Mo-MBGNs, and B-/Mo-MBGNs combinations, in order to identify genes and pathways differentially induced by the MBGNs in comparison to the untreated controls. By SAM, 93 differentially expressed genes were found in all MBGNs-exposed groups compared to the controls. Overrepresentation analysis for the Reactome pathway annotation set with the individual list of DEGs for each group detected three Reactome pathways: Cholesterol biosynthesis, ECM proteoglycans, and signaling by TGFB family members. Validation of the DEGs expression pattern of three identified Reactome pathways confirmed the results obtained by gene array analysis. PCR validation results also showed that Mo-MBGNs and the B-/Mo-MBGNs combinations outperformed MBGNs and B-MBGNs in modulating the expression of the DEGs, suggesting a stronger impact of Mo on gene expression. The identified genes coding for enzymes and molecules of the cholesterol biosynthesis, ECM proteoglycans and signaling of TGFB family members are known to modulate osteogenic marker expression. Therefore, future studies should focus on evaluating the exact role of the identified pathways and molecules in the context of osteogenic differentiation of osteoblast precursor cells. This will provide a deeper insight into the mechanisms underlying the behavior of osteoblasts in bone regenerative procedures using ion-releasing BGs.

Author statement

All listed authors in the submitted manuscript “Transcriptomic response of human mesenchymal stromal cells exposed to Boron- and Molybdenum-substituted mesoporous bioactive glass nanoparticles” made substantial contribution to the conception, design, data acquisition, or analysis, and approved the final version.

Ethics statement

Ethical approval for harvesting human bone marrow tissue and utilization of isolated human BMSCs within the purpose of this study was obtained by the responsible ethics committee of the Medical Faculty of the University of Heidelberg (S-340/2018).

6. CRediT authorship contribution statement

Elke Kunisch: Conceptualization, Data curation, Formal analysis, Investigation, Methodology, Validation, Visualization, Writing - original draft, Writing - review & editing. **Qaizar Nawaz:** Data curation; Investigation; Visualization; Roles/Writing - original draft; Writing - review & editing. **Tilman Walker:** Resources; Supervision; Writing - review & editing. **Tobias Renkawitz:** Funding acquisition, Resources, Writing - review & editing. **Aldo R. Boccaccini:** Funding acquisition, Conceptualization, Resources, Supervision, Writing - review & editing. **Fabian Westhauser:** Funding acquisition, Conceptualization, Project administration, Validation, Supervision, Writing - review & editing.

Declaration of Competing Interest

The authors declare that they have no known competing financial

interests or personal relationships that could have appeared to influence the work reported in this paper.

Acknowledgement

We gratefully acknowledge the financial support of the Deutsche Forschungsgemeinschaft (DFG), grant reference BO1191/26–1 and WE6654/2–1. We thank the Microarray Core Facility, German Cancer Research Center (DKFZ), for providing excellent Expression Profiling services.

Data availability

The data supporting the findings of this study are available from the corresponding author upon request.

References

[1] L.L. Hench, R.J. Splinter, W.C. Allen, T.K. Greenlee, Bonding mechanisms at the interface of ceramic prosthetic materials, J. Biomed. Mater. Res. 5 (6) (2004) 117–141.
[2] L.L. Hench, Chronology of bioactive glass development and clinical applications, N. J. Glass Ceram. 03 (02) (2013) 67–73.
[3] L.L. Hench, J.R. Jones, Bioactive glasses: frontiers and challenges, Front. Bioeng. Biotechnol. 3 (2015) 194.
[4] S. Kargozar, N. Lotfibakhshaiesh, J. Ai, A. Samadikuchaksaraie, R.G. Hill, P. A. Shah, P.B. Milan, M. Mozafari, M. Fathi, M.T. Joghataei, Synthesis, physico-chemical and biological characterization of strontium and cobalt substituted bioactive glasses for bone tissue engineering, J. Non-Cryst. Solids 449 (2016) 133–140.
[5] E. Jablonska, D. Horkavcova, D. Rohanova, D.S. Brauer, A review of in vitro cell culture testing methods for bioactive glasses and other biomaterials for hard tissue regeneration, J. Mater. Chem. B 8 (48) (2020) 10941–10953.
[6] K. Zheng, Y. Fan, E. Torre, P. Balasubramanian, N. Taccardi, C. Cassinelli, M. Morra, G. Iviglia, A.R. Boccaccini, Incorporation of boron in mesoporous bioactive glass nanoparticles reduces inflammatory response and delays osteogenic differentiation, Part. & Part. Syst. Charact. 37 (7) (2020).
[7] F. Westhauser, S. Wilkesmann, Q. Nawaz, F. Hohenbild, F. Rehder, M. Saur, J. Fellenberg, A. Moghaddam, M.S. Ali, W. Peukert, A.R. Boccaccini, Effect of manganese, zinc, and copper on the biological and osteogenic properties of mesoporous bioactive glass nanoparticles, J. Biomed. Mater. Res. A 109 (8) (2021) 1457–1467.
[8] E. Kunisch, L.A. Fiehn, M. Saur, M. Arango-Ospina, C. Merle, S. Hagmann, A. Stiller, L. Hupa, T. Renkawitz, A.R. Boccaccini, F. Westhauser, A comparative in vitro and in vivo analysis of the biological properties of the 45S5-, 1393-, and 0106-B1-bioactive glass compositions using human bone marrow-derived stromal cells and a rodent critical size femoral defect model, Biomater. Adv. 153 (2023) 213521.
[9] T.H. Qazi, J.C. Berkmann, J. Schoon, S. Geissler, G.N. Duda, A.R. Boccaccini, E. Lippens, Dosage and composition of bioactive glasses differentially regulate angiogenic and osteogenic response of human MSCs, J. Biomed. Mater. Res A 106 (11) (2018) 2827–2837.
[10] S. Decker, M. Arango-Ospina, F. Rehder, A. Moghaddam, R. Simon, C. Merle, T. Renkawitz, A.R. Boccaccini, F. Westhauser, vitro and in ovo impact of the ionic dissolution products of boron-doped bioactive silicate glasses on cell viability, osteogenesis and angiogenesis, Sci. Rep. 12 (1) (2022) 8510.
[11] I.D. Xynos, A.J. Edgar, L.D. Buttery, L.L. Hench, J.M. Polak, Ionic products of bioactive glass dissolution increase proliferation of human osteoblasts and induce insulin-like growth factor II mRNA expression and protein synthesis, Biochem Biophys. Res Commun. 276 (2) (2000) 461–465.
[12] I.D. Xynos, A.J. Edgar, L.D. Buttery, L.L. Hench, J.M. Polak, Gene-expression profiling of human osteoblasts following treatment with the ionic products of Bioglass 45S5 dissolution, J. Biomed. Mater. Res 55 (2) (2001) 151–157.
[13] I. Christodoulou, L.D. Buttery, G. Tai, L.L. Hench, J.M. Polak, Characterization of human fetal osteoblasts by microarray analysis following stimulation with 58S bioactive gel-glass ionic dissolution products, J. Biomed. Mater. Res B Appl. Biomater. 77 (2) (2006) 431–446.
[14] E.P. Ferraz, F.S. Oliveira, P.T. de Oliveira, M.C. Crovace, O. Peitl-Filho, M. M. Beloti, A.L. Rosa, Bioactive glass-based surfaces induce differential gene expression profiling of osteoblasts, J. Biomed. Mater. Res A 105 (2) (2017) 419–423.
[15] K.F. Bombonato-Prado, L.S. Bellesini, C.M. Junta, M.M. Marques, G.A. Passos, A. L. Rosa, Microarray-based gene expression analysis of human osteoblasts in response to different biomaterials, J. Biomed. Mater. Res A 88 (2) (2009) 401–408.
[16] H. Autefage, E. Gentleman, E. Littmann, M.A. Hedegaard, T. Von Erlach, M. O'Donnell, F.R. Burden, D.A. Winkler, M.M. Stevens, Sparse feature selection methods identify unexpected global cellular response to strontium-containing materials, Proc. Natl. Acad. Sci. USA 112 (14) (2015) 4280–4285.
[17] C. von Mering, M. Huynen, D. Jaeggi, S. Schmidt, P. Bork, B. Snel, STRING: a database of predicted functional associations between proteins, Nucleic Acids Res. 31 (1) (2003) 258–261.
[18] G. Dennis Jr., B.T. Sherman, D.A. Hosack, J. Yang, W. Gao, H.C. Lane, R. A. Lempicki, DAVID: database for annotation, visualization, and integrated discovery, Genome Biol. 4 (5) (2003) P3.
[19] P.D. Thomas, M.J. Campbell, A. Kejariwal, H. Mi, B. Karlak, R. Daverman, K. Diemer, A. Muruganujan, A. Narechania, PANTHER: a library of protein families and subfamilies indexed by function, Genome Res. 13 (9) (2003) 2129–2141.
[20] C. Migneco, E. Fiume, E. Verne, F. Baino, A guided walk through the world of mesoporous bioactive glasses (MBGs): fundamentals, processing, and applications, Nanomaterials 10 (12) (2020).
[21] D. Arcos, M.T. Portoles, Mesoporous bioactive nanoparticles for bone tissue applications, Int. J. Mol. Sci. 24 (4) (2023).
[22] K. Zheng, A.R. Boccaccini, Sol-gel processing of bioactive glass nanoparticles: a review, Adv. Colloid Interface Sci. 249 (2017) 363–373.
[23] M. Vallet-Regi, A.J. Salinas, Mesoporous bioactive glasses for regenerative medicine, Mater. Today Bio 11 (2021) 100121.
[24] S. Gupta, S. Majumdar, S. Krishnamurthy, Bioactive glass: a multifunctional delivery system, J. Control Release 335 (2021) 481–497.
[25] M. Moll, A. Scheurle, Q. Nawaz, T. Walker, E. Kunisch, T. Renkawitz, A. R. Boccaccini, F. Westhauser, Osteogenic and angiogenic potential of molybdenum-containing mesoporous bioactive glass nanoparticles: an ionic approach to bone tissue engineering, J. Trace Elem. Med Biol. 86 (2024) 127518.
[26] A. Scheurle, E. Kunisch, A.R. Boccaccini, T. Walker, T. Renkawitz, F. Westhauser, Boric acid and Molybdenum trioxide synergistically stimulate osteogenic differentiation of human bone marrow-derived mesenchymal stromal cells, J. Trace Elem. Med. Biol. 83 (2024) 127405.
[27] P. Balasubramanian, T. Büttner, V. Miguez Pacheco, A.R. Boccaccini, Boron-containing bioactive glasses in bone and soft tissue engineering, J. Eur. Ceram. Soc. 38 (3) (2018) 855–869.
[28] Q. Nawaz, M.A.U. Rehman, A. Burkovski, J. Schmidt, A.M. Beltran, A. Shahid, N. K. Alber, W. Peukert, A.R. Boccaccini, Synthesis and characterization of manganese containing mesoporous bioactive glass nanoparticles for biomedical applications, J. Mater. Sci. Mater. Med 29 (5) (2018) 64.
[29] D. Ege, Q. Nawaz, A.M. Beltran, A.R. Boccaccini, Effect of boron-doped mesoporous bioactive glass nanoparticles on C2C12 cell viability and differentiation: potential for muscle tissue application, ACS Biomater. Sci. Eng. 8 (12) (2022) 5273–5283.
[30] Q. Nawaz, G.B. López, T. Strunk, C. Damiani, C. Mas-Moruno, F. Westhauser, M. Michalek, N. Mutlu, A.R. Boccaccini, 3D printing of PCL-based composite scaffolds coated with mesoporous bioactive glass nanoparticles (MBGNs) incorporating boron and molybdenum for ion-assisted bone tissue engineering, J. Mater. Sci. 60 (19) (2025) 7924–7941.
[31] T.H. Qazi, S. Hafeez, J. Schmidt, G.N. Duda, A.R. Boccaccini, E. Lippens, Comparison of the effects of 45S5 and 1393 bioactive glass microparticles on hMSC behavior, J. Biomed. Mater. Res. Part A 105 (10) (2017) 2772–2782.
[32] P. Naruphontjirakul, O. Tsigkou, S. Li, A.E. Porter, J.R. Jones, Human mesenchymal stem cells differentiate into an osteogenic lineage in presence of strontium containing bioactive glass nanoparticles, Acta Biomater. 90 (2019) 373–392.
[33] J.H. Lee, N. Mandakhbayar, A. El-Fiqi, H.W. Kim, Intracellular co-delivery of Sr ion and phenamil drug through mesoporous bioglass nanocarriers synergizes BMP signaling and tissue mineralization, Acta Biomater. 60 (2017) 93–108.
[34] P. Naruphontjirakul, M. Li, A.R. Boccaccini, Strontium and zinc co-doped mesoporous bioactive glass nanoparticles for potential use in bone tissue engineering applications, Nanomaterials 14 (7) (2024).
[35] B. Widholz, S. Tsitlakidis, B. Reible, A. Moghaddam, F. Westhauser, Pooling of patient-derived mesenchymal stromal cells reduces inter-individual confounder-associated variation without negative impact on cell viability, proliferation and osteogenic differentiation, Cells 8 (6) (2019).
[36] B. Reible, G. Schmidmaier, A. Moghaddam, F. Westhauser, Insulin-like growth factor-1 as a possible alternative to bone morphogenetic protein-7 to induce osteogenic differentiation of human mesenchymal stem cells in vitro, Int. J. Mol. Sci. 19 (6) (2018).
[37] B. Reible, G. Schmidmaier, M. Prokscha, A. Moghaddam, F. Westhauser, Continuous stimulation with differentiation factors is necessary to enhance osteogenic differentiation of human mesenchymal stem cells in-vitro, Growth Factors 35 (4-5) (2017) 179–188.
[38] S. Wilkesmann, F. Westhauser, J. Fellenberg, Combined fluorescence-based in vitro assay for the simultaneous detection of cell viability and alkaline phosphatase activity during osteogenic differentiation of osteoblast precursor cells, Methods Protoc. 3 (2) (2020).
[39] E. Kunisch, S. Maenz, M. Knoblich, F. Ploeger, K.D. Jandt, J. Bossert, R.W. Kinne, S. Alsalameh, Short-time pre-washing of brushite-forming calcium phosphate cement improves its in vitro cytocompatibility, Tissue & Cell 49 (6) (2017) 697–710.
[40] A.I. Saeed, V. Sharov, J. White, J. Li, W. Liang, N. Bhagabati, J. Braisted, M. Klapa, T. Currier, M. Thiagarajan, A. Sturn, M. Snuffin, A. Rezantsev, D. Popov, A. Ryltsov, E. Kostukovich, I. Borisovsky, Z. Liu, A. Vinsavich, V. Trush, J. Quackenbush, TM4: a free, open-source system for microarray data management and analysis, BioTechniques 34 (2) (2003) 374–378.
[41] T. Metsalu, J. Vilo, ClustVis: a web tool for visualizing clustering of multivariate data using principal component analysis and heatmap, Nucleic Acids Res. 43 (W1) (2015) W566–W570.
[42] P.D. Thomas, D. Ebert, A. Muruganujan, T. Mushayahama, L.-P. Albou, H. Mi, 2022, PANTHER: Making genome-scale phylogenetics accessible to all, 31(1) 8-22.

[43] T. Attin, K. Becker, C. Hannig, W. Buchalla, R. Hilgers, Method to detect minimal amounts of calcium dissolved in acidic solutions, Caries Res 39 (5) (2005) 432–436.
[44] T. Attin, K. Becker, C. Hannig, W. Buchalla, A. Wiegand, Suitability of a malachite green procedure to detect minimal amounts of phosphate dissolved in acidic solutions, Clin. Oral. Invest. 9 (3) (2005) 203–207.
[45] M. Dziadek, B. Zagrajczuk, P. Jelen, Z. Olejniczak, K. Cholewa-Kowalska, Structural variations of bioactive glasses obtained by different synthesis routes, Ceram. Int. 42 (13) (2016) 14700–14709.
[46] S.R. Gavinho, A.S. Padua, I. Sa-Nogueira, J.C. Silva, J.P. Borges, L.C. Costa, M.P. F. Graca, Fabrication, structural and biological characterization of zinc-containing bioactive glasses and their use in membranes for guided bone regeneration, Materials 16 (3) (2023).
[47] W. Niu, Y. Guo, Y. Xue, M. Chen, M. Wang, W. Cheng, B. Lei, Monodisperse branched molybdenum-based bioactive nanoparticles significantly promote osteogenic differentiation of adipose-derived stem cells, Part. Part. Syst. Charact. 36 (7) (2019).
[48] S. Decker, E. Kunisch, A. Moghaddam, T. Renkawitz, F. Westhauser, Molybdenum trioxide enhances viability, osteogenic differentiation and extracellular matrix formation of human bone marrow-derived mesenchymal stromal cells, J. Trace Elem. Med. Biol. 68 (2021) 126827.
[49] M.M. Dvorak, A. Siddiqua, D.T. Ward, D.H. Carter, S.L. Dallas, E.F. Nemeth, D. Riccardi, Physiological changes in extracellular calcium concentration directly control osteoblast function in the absence of calciotropic hormones 101 (14) (2004) 5140–5145.
[50] H. Dry, K. Jorgenson, W. Ando, D.A. Hart, C.B. Frank, A. Sen, Effect of calcium on the proliferation kinetics of synovium-derived mesenchymal stromal cells, Cytotherapy 15 (7) (2013) 805–819.
[51] A. Suzuki, M. Minamide, C. Iwaya, K. Ogata, J. Iwata, Role of metabolism in bone development and homeostasis, Int. J. Mol. Sci. 21 (23) (2020).
[52] X.-Y. Dong, S.-Q. Tang, J.-D. Chen, Dual functions of Insig proteins in cholesterol homeostasis, Lipids Health Dis. 11 (1) (2012) 173.
[53] H. Li, H. Guo, H. Li, Cholesterol loading affects osteoblastic differentiation in mouse mesenchymal stem cells, Steroids 78 (4) (2013) 426–433.
[54] L. You, Z.Y. Sheng, C.L. Tang, L. Chen, L. Pan, J.Y. Chen, High cholesterol diet increases osteoporosis risk via inhibiting bone formation in rats, Acta Pharm. Sin. 32 (12) (2011) 1498–1504.
[55] A. Suzuki, K. Ogata, H. Yoshioka, J. Shim, C.A. Wassif, F.D. Porter, J. Iwata, Disruption of Dhcr7 and Insig1/2 in cholesterol metabolism causes defects in bone formation and homeostasis through primary cilium formation, Bone Res. 8 (2020) 1.
[56] A.B. Ouweneel, M.J. Thomas, M.G. Sorci-Thomas, The ins and outs of lipid rafts: functions in intracellular cholesterol homeostasis, microparticles, and cell membranes: thematic review series: biology of lipid rafts, J. Lipid Res. 61 (5) (2020) 676–686.
[57] E. Wei, M. Hu, L. Wu, X. Pan, Q. Zhu, H. Liu, Y. Liu, TGF-beta signaling regulates differentiation of MSCs in bone metabolism: disputes among viewpoints, Stem Cell Res Ther. 15 (1) (2024) 156.
[58] K.M. Nicks, D.S. Perrien, N.S. Akel, L.J. Suva, D. Gaddy, Regulation of osteoblastogenesis and osteoclastogenesis by the other reproductive hormones, Activin and Inhibin, Mol. Cell Endocrinol. 310 (1-2) (2009) 11–20.
[59] Y. Kanno, The roles of fibrinolytic factors in bone destruction caused by inflammation, Cells 13 (6) (2024).
[60] S. Ikegawa, Expression, regulation and function of asporin, a susceptibility gene in common bone and joint diseases, Curr. Med. Chem. 15 (7) (2008) 724–728.
[61] L. Xu, Z. Li, S.Y. Liu, S.Y. Xu, G.X. Ni, Asporin and osteoarthritis, Osteoarthr. Cartil. 23 (6) (2015) 933–939.
[62] J. Sun, T. Zhang, P. Zhang, L. Lv, Y. Wang, J. Zhang, S. Li, Overexpression of the PLAP-1 gene inhibits the differentiation of BMSCs into osteoblast-like cells, J. Mol. Histol. 45 (5) (2014) 599–608.
[63] R.M. Hughes, B.W. Simons, H. Khan, R. Miller, V. Kugler, S. Torquato, D. Theodros, M.C. Haffner, T. Lotan, J. Huang, E. Davicioni, S.S. An, R.C. Riddle, D.L.J. Thorek, I.P. Garraway, E.J. Fertig, J.T. Isaacs, W.N. Brennen, B.H. Park, P.J. Hurley, Asporin restricts mesenchymal stromal cell differentiation, alters the tumor microenvironment, and drives metastatic progression, Cancer Res. 79 (14) (2019) 3636–3650.
[64] S. Liu, X. Yan, J. Guo, H. An, X. Li, L. Yang, X. Yu, S. Li, Periodontal ligament-associated protein-1 knockout mice regulate the differentiation of osteoclasts and osteoblasts through TGF-beta1/Smad signaling pathway, J. Cell Physiol. 239 (3) (2024) e31062.
[65] M. Sillen, P.J. Declerck, A narrative review on plasminogen activator inhibitor-1 and Its (Patho)Physiological role: to target or not to target? Int. J. Mol. Sci. 22 (5) (2021).
[66] Y. Takafuji, K. Tatsumi, M. Ishida, N. Kawao, K. Okada, O. Matsuo, H. Kaji, Plasminogen activator inhibitor-1 deficiency suppresses osteoblastic differentiation of mesenchymal stem cells in mice, J. Cell Physiol. 234 (6) (2019) 9687–9697.